



ELSEVIER

Contents lists available at ScienceDirect

Ad Hoc Networks

journal homepage: www.elsevier.com/locate/adhoc

Statistical wireless channel propagation characteristics in underground mines at 900 MHz: A comparative analysis with indoor channels

Khalid A. Qaraqe^a, Serhan Yarkan^{b,*}, Sabih Güzelgöz^c, Hüseyin Arslan^c

^a Department of Electrical and Computer Engineering, Texas A & M University at Qatar, Texas A & M Engineering Building, Education City, Doha 23874, Qatar

^b Electrical and Computer Engineering, Texas A & M University, Wisenbaker Research Building, Bizell St., College Station, TX 77843, United States

^c Department of Electrical Engineering, University of South Florida, 4202 E. Fowler Avenue, ENB-118, Tampa, FL 33620, United States

ARTICLE INFO

Article history:

Available online xxxx

Keywords:

Antenna heights

Indoor

Path loss

Radio propagation

Statistical parameters

Underground mine

ABSTRACT

This work investigates the wideband characterization of radio propagation channel for an active, real underground mine environment. Important statistical parameters related to path loss, delay, and amplitude characteristics are extracted. Impact of different antenna heights on path loss exponent is investigated. The same measurement procedure is performed to extract the statistical characteristics of a university building due to the structural similarities between the two environments since both include long hallways, crosscuts, and turns. Based on the results, a comparative analysis is presented along with concluding remarks and future directions.

© 2011 Elsevier B.V. All rights reserved.

1. Introduction

Telecommunications can broadly be divided into the following two categories: wired and wireless communication. Wired communication, as its name implies, aims to transmit signals over such a medium consisting of conducting metals as wires that physically connect two communicating nodes. In contrast to wired transmission, wireless transmission strives to achieve the same goal without a physical connection between the communicating nodes.¹ Therefore, it is valid to state that the difference between wired and wireless communications is the propagation environment over which the signals are transmitted.

Propagation environment in wireless communication is highly dynamic compared to that in wired communication because of mobility of the communicating nodes and/or of objects within the environment. In addition, propagation characteristics change drastically from environment to environment due to the inherent nature of wave propagation mechanisms. Having a highly dynamic environment along with environment-dependent propagation mechanisms mandates one to understand and characterize the behavior of the signal transmission over wireless channels. Therefore, characterization of wireless channels lies in the heart of developing reliable and successful communication systems.

Studies to characterize the wireless radio propagation channels of indoor environments have been numerous in recent years, especially given the success of cellular technology, wireless local area networks (WLANs) and other demands on wireless technology. Those studies include the characterization of radio propagation in various environments such as office buildings [1,2], university halls [3], factories [4], laboratory buildings [5], and so on. After some recent tragic events occurred in underground mines, the use of wireless communications in these environments is being considered as well.

* Corresponding author. Tel.: +1 713 2801987; fax: +1 979 8458986.

E-mail addresses: kqaraqe@tamu.edu (K.A. Qaraqe), syarkan@ece.tamu.edu (S. Yarkan), guzelgo@mail.usf.edu (S. Güzelgöz), arslan@eng.usf.edu (H. Arslan).

¹ It is important to note that in some sort of radio communication systems, the two communicating nodes might not be physically connect to each other but still have some conducting materials in between to facilitate the propagation. Leaky feeder systems that are heavily used in underground mines can be considered one of the examples of such hybrid schemes.

Wireless communication is of great importance for underground mines from several perspectives including safety, security, and industry. It is used in underground mines in several ways such as communicating between in-mine locations and ground (surface) stations, remote sensing and controlling of equipment and devices, and tracking machinery and miners. Moreover, wireless communication provides significant reductions in maintenance, since it allows transmission without wires in these harsh environments.

Underground mines are very distinct environments in terms of behavior of radio propagation. Furthermore, normal operations in underground mines share similarities to disaster communications. Therefore, understanding wireless solutions in mining gives insight into problems and solutions for disaster communications as well [6].

It can be said that the general use of wireless communications in underground mines began in the first half of the previous century [7]. Early studies focused on TTE communications [8–10] and were based mainly on theoretical approaches. Although TTE is extremely important for underground mine communications, a complete communication system for mines not only consists of sending radio signals to the ground, but also includes in-gallery communications. Hence, characteristics of radio propagation in underground mine tunnels were studied as well. Early researchers tried to model the behavior of propagation in mines by studying the characteristics of regular tunnels in UHF bands [11,12]. It is understood in this regard that the shapes of mine galleries such as curved tunnels and structures of mine walls must also be taken into account [11,13].

Unlike the theoretical approaches, empirical approaches are not widely available in the literature due to the arduous work involved, difficult to obtain permissions, and safety restrictions. However, recently, empirical approaches in underground mines have attracted a significant attention because of some unfortunate accidents. This increasing attention has provided researchers with opportunities to characterize the wireless channels of underground mines in detail. It is difficult to classify the empirical studies conducted, because the propagation characteristics and ground structures are not distinguishing properties of mines. A coarse classification is still possible by looking at the spectrum used in the measurements. In [14], measurements are reported for several transmission frequencies, *i.e.*, 200, 415, and 1000 MHz, in the presence of obstructions such as pillars. With the increase in demand for high-data rate communications, earlier measurements need to be repeated for wider bandwidths. Some results from the perspective of a 1 Mbps wireless network for a mine that includes rooms and pillars are presented in [15,16]. Other wideband measurement sets can be found in [17–20].

Even though underground mines are extreme environments, there are still some structural similarities to more typical scenarios, especially to indoor environments. Long corridors and intersections where there occasionally exists LOS transmission are the major common structural similarities of both environments. These similarities suggest

the idea of comparing these two environments. This paper therefore compares the radio propagation in regular indoor and mine environments. Due to its good propagation characteristics in regular environments and popular use, 850–950 MHz radio spectrum band is selected for measurements. The main contributions of the paper are as follows: CI important statistical parameters of the radio channel are provided for both environments by employing the same measurement equipment and procedure in order to compare the results with each other. In addition, signal power measurements and other results are given for special structures such as curvatures and U-turns since the behavior of the wireless signal for these structures is extremely important.² Moreover, considering the possibility of the use of robots for wireless transmission in such environments, special setups which simulate (especially for disaster scenarios) robot-to-robot and robot-to-human communications are designed and corresponding measurement results are presented. To the best knowledge of authors, this study provides one of the first measurement results which are obtained by different antenna height combinations in underground mines. The organization of the rest of the paper is as follows: Section 2 outlines how the wireless propagation channel is characterized statistically. Sections 3 and 4 provide details of the measurements and their results for underground mine and for indoor experiments, respectively. Section 5 focuses on comparative analysis especially for path loss measurements in turning corridors and Section 6 concludes the paper.

2. Statistical characterization of the wireless propagation channel

Statistical characterization of wireless propagation channel is twofold: (i) establishing a mathematical model which describes the channel and performing sets of measurements through which relevant model parameters can be extracted. Mathematical model represents the physical phenomena as close (and preferably simple) as possible, whereas measurements allow one to quantify what the model describes.

2.1. Mathematical model

When a wireless signal is transmitted, the signal received at the receiver consists of attenuated, delayed, and phase-shifted replicas of the transmitted signal. Therefore, a complete characterization of the wireless channel can be given by its complex baseband impulse response as follows:

$$h(t, \tau) = \sum_{r=1}^{N(t)} a_r(t) e^{j\theta_r(t)} \delta(\tau - \tau_r(t)), \quad (1)$$

where $N(t)$ represents the number of resolvable multipath components at time t , $a_r(t)$ is the amplitude of the r th mul-

² Note that, in this study, although U-turn includes turns which can be considered as curvatures, we make the following distinction between these two structures: U-turn includes two curvatures which form a “U” shape, whereas a curvature refers to an arc-shaped structure.

tipath component, $\theta_r(t)$ denotes the phase, $\tau_r(t)$ represents the arrival time, and $\delta(\cdot)$ is the Dirac delta function. The frequency domain counterpart of (1) is given by:

$$H(t, f) = \sum_{r=1}^{N(t)} a_r(t) e^{-j(2\pi f \tau_r(t) - \theta_r(t))}. \quad (2)$$

Since (1) (and therefore, (2)) represents the channel for a fixed transmitter–receiver pair, channel impulse responses (CIRs) are collected in the vicinity of a local area to characterize the behavior of the wireless channel statistically. In order to remove the time dependency of CIRs, a time-invariant multipath PDP is calculated by means of an averaging over the local area of interest. Specifically, we can define a PDP around a given point as [21]:

$$P(\tau) = E\{|h(\tau)|^2\} \quad (3)$$

where $E\{\cdot\}$ is an expectation over local space. From the PDP, some of the very important parameters of the wireless channel of interest can be extracted as will be discussed in the subsequent section.

2.2. Measurement methodology and extracting statistical parameters

In order to collect data for extracting parameters related to the mathematical model, VNA measurements were performed for the frequency interval 850–950 MHz. This interval was measured using omnidirectional Anritsu 2000-1035 antennas. MT 8222 A BTS Master, which has multiple operation modes, was used as the VNA. Each spectral measurement was represented with 551 equally spaced frequency points (data points) within the interval specified by the VNA. Therefore, a spectral resolution of 0.181 MHz was obtained. The transmit power of the VNA was set to the maximum of the device, that is 0 dBm with an input amplification of 10 dBm. Next, the measurement system including connectors and cables was calibrated to remove the impairment caused by the components. The calibration data were saved both into the internal memory of the MT 8222 A and an external USB storage device. Then, the device removed the calibration data from the measurement by using its internal memory and provided S_{21} parameter in complex number format with real and imaginary parts for each data point.

Upon the collection of data, the following important statistical parameters were extracted for both underground mine and indoor environments:

2.2.1. Distance dependent path loss

The path loss exponent is determined by considering the total received power at each distance, averaged locally over space. For a specific distance d , the total received power is calculated as:

$$P_R(d) = \frac{1}{F \times L} \sum_{i=1}^F \sum_{j=1}^L |H(f_i, t_j; d)|^2, \quad (4)$$

where F denotes the number of data points (which is 551) and L denotes the number of local measurements at a specific distance d . Defining path loss as a decibel ratio of

transmit power to $P_R(d)$, and considering the decaying nature of the received power with path distance, we use the following familiar model for path loss, PL :

$$10 \times \log_{10} \left(\frac{P_T}{P_R(d)} \right) = A + 10 \times n \times \log_{10}(d), \quad (5)$$

where P_T is the transmit power in Watt, d denotes the transmitter–receiver separation in meter, A is called the intercept, and n is the path loss exponent.

2.2.2. Frequency dependent path loss

Generally, path loss increases as the transmission frequency increases. The relationship between path loss and frequency is often given by $(PL(f) \propto f^\kappa)$, where κ denotes the dependency and $PL(f)$ is spatially averaged to remove the small-scale effects [22].

2.2.3. Delay characteristics

As introduced in Section 2.1, the core of wireless propagation, which also includes delay characteristics, lies beneath CIR. However, VNA measurements can provide CTF rather than CIR. After the complex CTF is taken from the VNA, the IFT is applied and the complex CIR is obtained. By using the reasoning explained in Section 2.1, the PDP of a local area is calculated. With the aid of PDP, some very important statistical parameters such as maximum excess delay and RMS delay spread can be obtained.

At this point, it is worth mentioning some of the critical parameters of the equipment used in measurements and post-processing stages. When the measurement data were evaluated with the aid of an IFT operation, a sampling time of 10 ns (inverse of 100 MHz) is obtained in the time domain. Since there are 551 data points, the longest delay of a multipath that can be observed corresponds to 5.51 μ s. Two samples of CIRs which were obtained from indoor VNA measurements are presented in Fig. 1 for a straight corridor. As can be seen from Fig. 1, the received multipath power decays earlier than 5.51 μ s, which implies that these parameter settings are long enough to detect the major multipath components of the channel. In Fig. 1, note also that the relative received powers from the multipaths are normalized. This enables us to compare them with each other even though their amplitude scales are different. For instance, consider the two measurements as shown in Fig. 1, which were taken 18 m apart. If the peaks of CIRs are examined, it can be seen that the peak of the farther point is six samples ahead of the closer one. Because the sampling interval is 10 ns, the distance between two measurement points is found to be approximately 18 m ($6 \times (10 \text{ ns}) \times (3 \times 10^8 \text{ m/s})$), which confirms the delay characteristics of the CIRs.

Next, the CIRs were normalized in such a way that the area under each of them became unity. The delay spread statistics are calculated by considering several “cutoff thresholds.” The cutoff threshold is the number of dB below the peak return beyond which CIR terms are considered to be noise, and thus to be neglected. In the literature, 20 dB is the most prominent value [21,17].

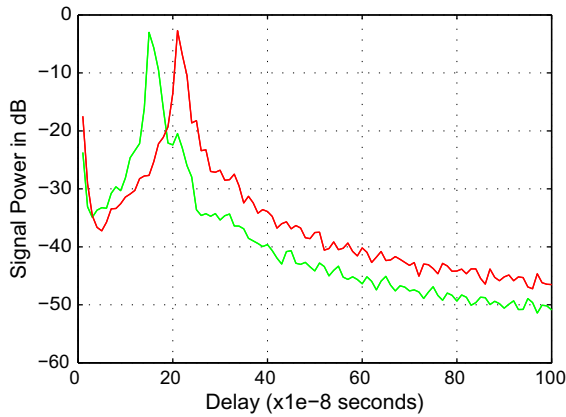


Fig. 1. Two instances of CIRs measured at 5.5 m and 23.5 m, respectively.

Therefore, a cutoff threshold of 20 dB was used in our calculations.

After applying the cutoff threshold so determined, paths that are below the threshold are set to zero, *i.e.*, not considered in the follow-on stages. Finally, the propagation delay for each CIR is shifted in delay so that the first significant return is at $\tau = 0$. Based on these settings, the maximum excess delay (τ_{\max}), and RMS delay spread (τ_{rms}) and their relative statistics were obtained as described in [21].

2.2.4. Path amplitude statistics

Another important statistical aspect of the channel is the distribution of the path amplitudes. Path amplitude statistics provide information about fading behavior of the channel and help design better performing receivers. For the sake of clarity, the statistical property presented here is the amplitude distribution of the first arriving paths, for both LOS and NLOS measurements in both environments. In order to model the statistical behavior properly, a distribution fit is required. Hypothesis testing was applied with the χ^2 test for the distribution fit. Test statistics were obtained for several candidate theoretical distributions for mobile radio channels such as Rayleigh, Rice, log-normal, Gamma, and Weibull [22]. The χ^2 test was chosen to be:

$$Q^2 = \sum_{r=1}^R \frac{(N_r - T_r)^2}{T_r}, \quad (6)$$

where R is the total number of bins, N_r is the number of samples in the r th bin, T_r denotes the corresponding theoretical frequency that occurs within the r th bin. In order to apply the χ^2 test, degrees of freedom must be determined appropriately, since it is important in evaluating the confidence interval. In the χ^2 test, degrees of freedom is $R - 1 - \phi$, where ϕ is the number of parameters estimated from the data. Then, the test statistic obtained from (6) is compared to the right tail of $\chi_{R-1-\phi}^2$ in case a confidence level is to be determined.

3. Underground mine experiment

3.1. Measurement environment

Mine measurements were performed in an active coal mine, Jim Walter Resources Inc., mine number 4, in Brookwood, Alabama. The shaft depth of the mine is approximately 610 m. It covers a vast area with many crosscuts, escape ways, first-aid stations, and blockages. Many hallways have railroads on the ground inside the mine. Some places inside, which are away from the main entrance, have water on the ground as well. The ground is not flat. The walls are rough and covered with lime powder to avoid explosions due to the presence of explosive gases. Some parts of the walls and ceilings are fortified with metal and wooden grids. The structure of the mine is not uniform. The average height of the mine is 2.5 m and the average width is 5.5 m. A descriptive digital picture of the underground mine environment is given in Fig. 2.

3.2. Measurement procedure

The VNA was placed onto a platform. The transmitter antenna was located on the VNA at a particular height. The receiver antenna was stabilized and set by a tripod. Three transmitter–receiver height combinations, namely 1.3–1.3 m, 1.3–0.4 m, and 0.4–0.4 m were tested. Height combinations were chosen very carefully to replicate a possible communication between devices which were carried on belt level as well as between robots.³ In this case, 1.3–1.3 m corresponds to belt-to-belt communications and will be referred in the remainder of the paper as “high transmitter–high receiver” combination; 1.3–0.4 m corresponds to belt-to-robot communications and will be referred in the remainder of the paper as “high transmitter–low receiver” combination; and 0.4–0.4 m corresponds to robot-to-robot communications and will be referred in the remainder of the paper as “low transmitter–low receiver” combination. Cable and connector connections were established for the remaining part of the measurement procedure.

Measurements were taken for specific transmitter–receiver separations. In the mine, six local measurements were performed for each transmitter–receiver separation. This was achieved by splitting the width of the mine tunnels into approximately six equal pieces due to non-uniform structure of the tunnels. Because of the uneven width and rough wall structure, the receiver antenna (on its tripod) was kept at almost 0.5 m away from each side of the mine walls. After completing six measurements for a specific distance, the receiver antenna was moved (by Δd) to the next distance for another six local measurements. The reference distance, d_0 , and the distance between any two measurement points, Δd , were taken as 1 m and 1.5 m, respectively. The only exception for d_0 was in the curvature measurement where it was set to 3 m. Because of time limitations, only one measurement per height per distance was performed in the curvature measurements. Only straight corridors were considered

³ This sort of scenario can be very useful in search and rescue missions.

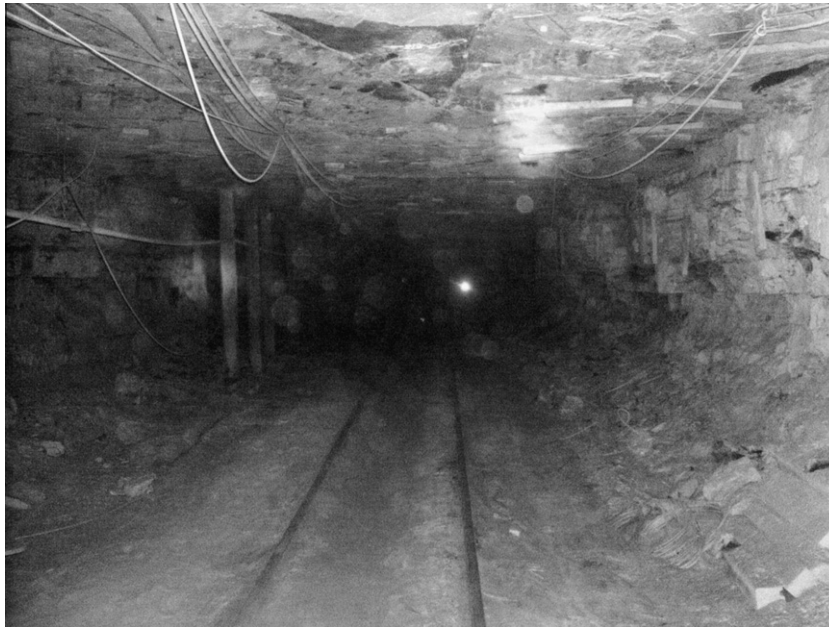


Fig. 2. An inside view of the mine galleries.

with one measurement per distance for the low transmitter–low receiver antenna combination due to the same access restrictions. These two (*i.e.*, curvature and low transmitter–low receiver antenna combination) measurements were particular to the mine and not performed in the indoor environment. A chart which summarizes measurement types and distance per number of measurements is given in Table 2. In total, four different locations were measured in the mine. The majority of the measurements were done in straight tunnels, which correspond to LOS cases. Illustrations of the measurements for underground mine environment are presented in Fig. 3. All measurements were taken without any human or other activity and with stationary transmitter, so we can assume that the channel was time-invariant over the duration of each measurement.

3.3. Measurement results

This section presents several important statistical parameters extracted from the measurement data. It should be noted that the horizontal axis in straight corridor path loss measurement plots in both environments (*i.e.*, the mine and the indoor), is given in a logarithmic scale ($10\log_{10}(d/d_0)$), whereas it is given as index points in the other (*i.e.*, curvature and U-turn) path loss measurement plots. This difference in representation stems from the fact that in curvature and U-turn measurements, two distances can be defined: (1) Euclidean distance, and path distance which corresponds approximately to the length of the cable connecting the receiver to the VNA. In order to avoid confusion, measurement point indices are used in presenting the path loss results for curvature and U-turn tests.

For the measurements performed in the mine, Figs. 4–6 present the path loss versus distance. In order to extract

the path loss exponent, linear regression was applied to the data obtained from measurements. For the mine environment, n was found to be 2.00 with a standard deviation of 0.15 for the high transmitter–high receiver antenna combination. An instance of the measurement data is plotted in Fig. 4. In [23], we have applied the same measurement procedure with the same measurement equipment and setup in Bruceton Mine, Pittsburgh, Pennsylvania, USA yielding a mean path loss exponent of 1.82. In the literature, the path loss exponent for 2.4 GHz is found to be 2.10 [18], and for 5.8 GHz it is found to be 2.30 [17]. In this regard, the findings bear high resemblance to the ones reported in the literature for the same kind of underground mine structures.

In addition to measurement procedure encountered in the literature frequently, high transmitter–low receiver antenna combination measurements were also performed and the n was computed to be 1.33. Within the same environment, it is observed that the n for the high transmitter–low receiver antenna combination is lower than the former one. It is noteworthy that high transmitter–low receiver antenna combination measurements are not vast in the literature for underground mines. Therefore, it is very difficult for the authors to draw a general conclusion about the relationship between n and antenna height. This issue will be discussed in Section 5 from a different perspective as well.

Path loss measurement in underground mine was performed for the low transmitter–low receiver combination too. However, due to time restrictions on mine access, enough statistics could not be collected for the low transmitter–low receiver combination. Therefore, the authors avoid making any general comments regarding the measurements of this combination. Yet, one set of the results of the measurements performed are given in [24]. Path loss

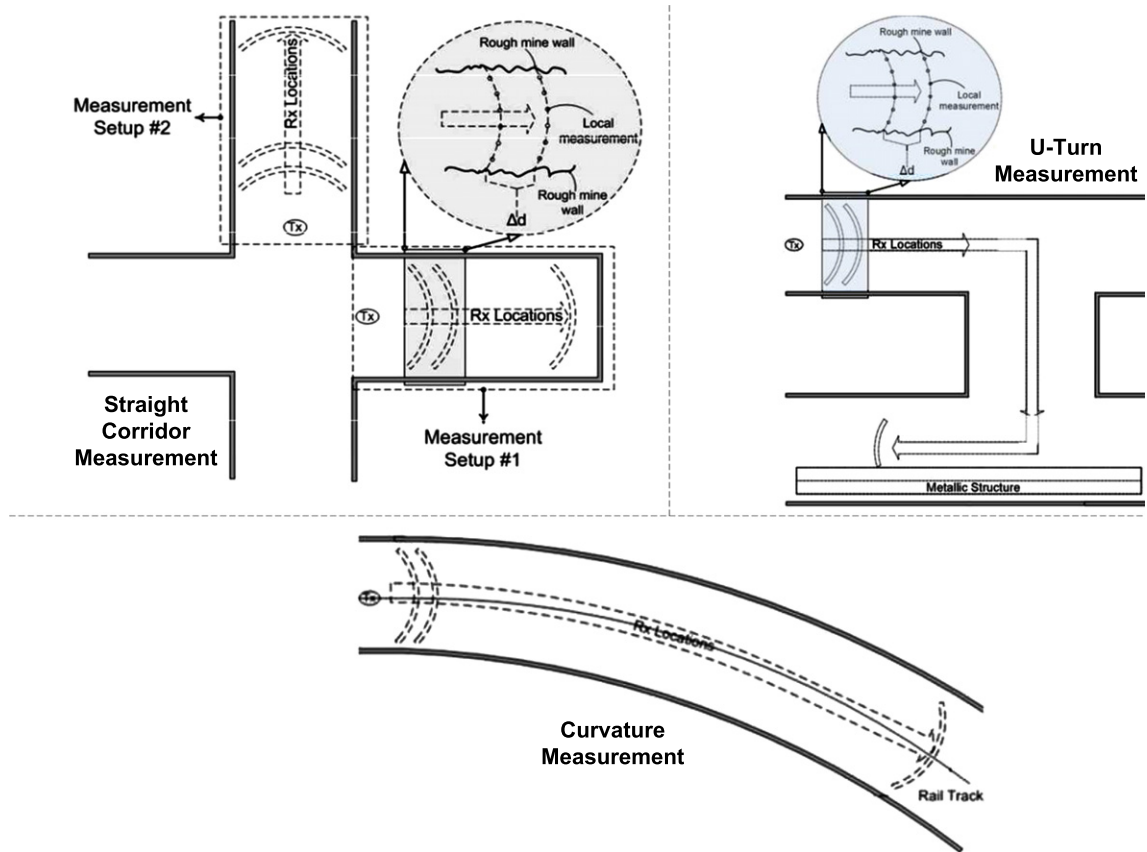


Fig. 3. Three setups for straight corridor, U-turn, and curvature measurements in the underground mine environment.

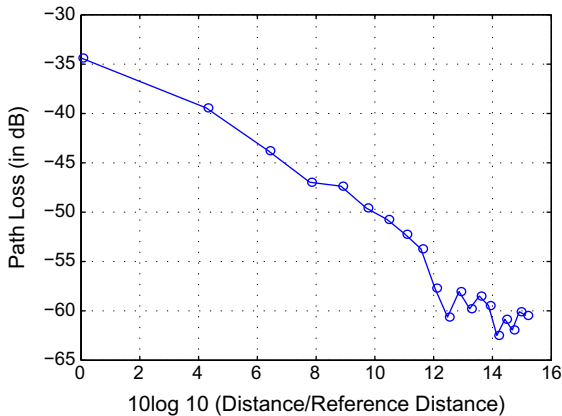


Fig. 4. Mine path loss measurement results and the estimation of path loss exponent for 1.3–1.3 m antenna height combination. $n = 2.17$ is found by applying least squares estimation.

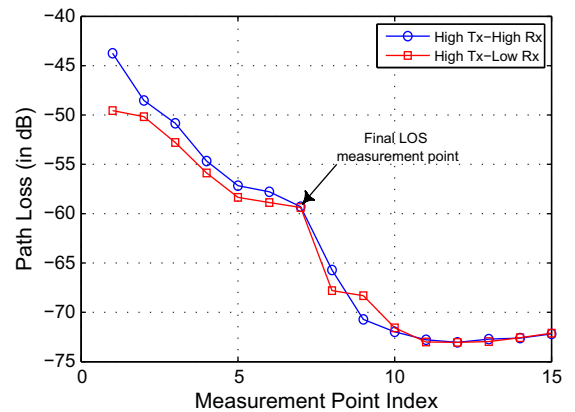


Fig. 5. Mine U-turn measurement results with 1.3–1.3 m and 1.3–0.4 m antenna height combinations. Note that there is a 6 dB and 8 dB loss between 7th and 8th measurement point reflecting the impact of turns on signal power for 1.3–1.3 m and 1.3–0.4 m antenna height combinations, respectively. This drastic loss is seen on the same point for both antenna combinations, because 7th point corresponds to last LOS measurement, whereas 8th point corresponds to the first measurement as soon as the first turn is made.

results for U-turn measurements with high transmitter–high receiver and high transmitter–low receiver antenna combinations are given in Fig. 5. Also, results for curvature measurements with high transmitter–high receiver and high transmitter–low receiver antenna combinations are both given in Fig. 6. Relevant discussions for these results are left to Section 5.

From our data, κ was calculated to be 10^{-4} , which can be interpreted as there is no frequency-dependent path loss in the mines over the 850–950 MHz band measured.

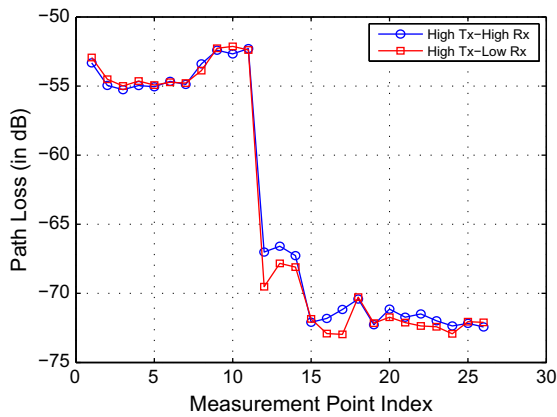


Fig. 6. Mine curvature measurement results for both 1.3–1.3 m and 1.3–0.4 m antenna height combinations.

Maximum excess delay was calculated to be 430 ns and the average RMS delay spread was found to be 39.34 ns. These statistics are consistent with the results in [23,18]. However, as stated in [18] the structure of the mine in which measurements are taken plays an important role in some temporal characteristics.

Following the procedure described earlier, amplitude distribution of the first arriving paths for LOS and NLOS measurements in the mine is tabulated in Table 1.1 and 1.2. For LOS measurements in the mine, the Rice distribution fits best, *i.e.*, has the lowest among all test statistic values as can be seen from Table 1.1. The Weibull and Gamma distributions are the next best candidate distributions. For NLOS measurements in the mine, the relevant test statis-

Table 1
 χ^2 test results of comparison of specific theoretical distributions to the empirical data.

Distribution	Test stat. (Q^2)	Pr(acceptance of hypothesis)
<i>Table 1.1: Results of LOS for mine measurements</i>		
Rayleigh	6.84	0.74
Rice	4.81	0.94
Log-normal	6.17	0.80
Gamma	5.16	0.88
Weibull	5.57	0.85
<i>Table 1.2: Results of NLOS for mine measurements</i>		
Rayleigh	3.94	0.95
Rice	9.02	0.62
Log-normal	6.51	0.77
Gamma	5.31	0.87
Weibull	5.01	0.89
<i>Table 1.3: Results of LOS for indoor measurements</i>		
Rayleigh	3.62	0.96
Rice	1.85	0.99
Log-normal	3.72	0.95
Gamma	3.21	0.97
Weibull	0.47	1.00
<i>Table 1.4: Results of NLOS for indoor measurements</i>		
Rayleigh	0.31	1.00
Rice	2.30	0.99
Log-normal	11.8	0.29
Gamma	1.10	0.99
Weibull	0.90	0.99

Table 2

Measurement chart for the underground mine experiments (measurement/distance [m/d]).

Structure	Tx-Rx		
	1.3–1.3 m	1.3–0.4 m	0.4–0.4 m
Straight	6 m/d and 1 m/d	1 m/d	6 m/d
U-turn	6 m/d	6 m/d	–
Curvature	1 m/d	1 m/d	–

tics are given in Table 1.2. It is seen there that the Rayleigh distribution fits best, *i.e.*, has the lowest of the test statistic values; and the Gamma and Weibull distributions are the next best candidates. These amplitude distributions in both LOS and NLOS are reported to be the best candidates in [23] as well.

4. Indoor experiment

4.1. Measurement environment

Regular indoor measurements were carried out on the third floor of the Electrical Engineering building of the University of South Florida (USF), Tampa, FL. The inner walls are made of concrete blocks. However, there are some wooden doors opening to laboratories and offices. The ceiling is made of plywood. The floor is tiled with marble. The height and width of the corridors are both 2.5 m. A descriptive digital picture of the indoor environment is presented in Fig. 7.

4.2. Measurement procedure

Indoor measurements were carried out in a similar way to the ones performed in underground mine. Antenna heights, the procedure, and the devices used were all the same with some minor differences. Since the indoor corridors are structurally more even compared to those of underground mines, seven local measurements at each distance were carried out. The reference distance for all of the measurements, d_0 , was approximately 1 m, and the distance between any two consecutive measurement points, Δd , was determined by considering the length of the corridors which varied between 1.5 m and 3.0 m. The statistics of indoor environment were obtained from four different measurement locations in total.

4.3. Measurement results

In order to extract n for the measurements performed in indoor environment, linear regression was applied to the data. For the regular indoor environment, n for both antenna height combinations was found to be almost the same, unlike the case observed in the mine. The mean path loss exponent for the high transmitter–high receiver antenna combination was calculated to be 1.50 with a standard deviation of 0.4 out of all of the measurement locations. Values obtained for the high transmitter–low receiver antenna combination implied that the mean path loss exponent is to be 1.65 with a standard deviation of 0.35. This



Fig. 7. Descriptive picture of the indoor environment.

reveals that antenna height does not impact the path loss statistics significantly for indoor environments, which conforms with previous studies presented in the literature for wideband measurement results [25,26]. Furthermore, observing a path loss exponent which is lower than 2 (i.e., path loss exponent for free space) provides a strong evidence for waveguide effect due to architectural regularity and surface structure of hallways [27–29]. Path loss results for U-turn measurements with high transmitter–high receiver and high transmitter–low receiver antenna combinations are given in Figs. 8 and 9, respectively. The detailed comparative analysis of the results will be given in Section 5.

As in underground mine case, κ was calculated to be 10^{-4} , which can be interpreted as there is no frequency-

dependent path loss in the university building over the 850–950 MHz band measured.

For indoor measurements, average maximum excess delay was calculated to be 240 ns while the average RMS delay spread was found to be 23.15 ns over all measurement locations. In [3], the RMS delay spread was estimated for several buildings of Columbia University. It was observed that RMS delay spread was under 100 ns for most of the locations. Similar measurements are reported in [28] where the RMS delay spread is found to be less than 22 ns with LOS and less than 55 ns with OLOS for most of the measurement locations. We observed also that RMS delay spread values for LOS condition are always the lowest which is consistent with the literature [28].

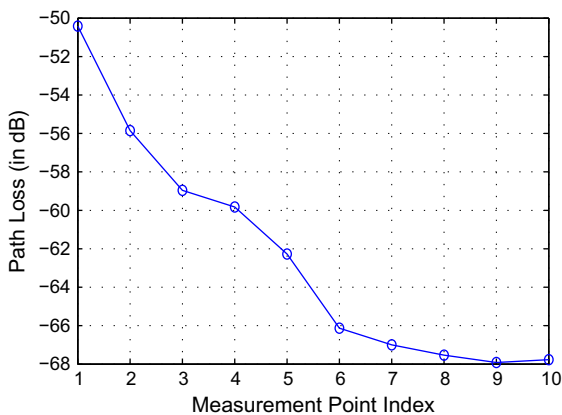


Fig. 8. Indoor U-turn path loss measurement results with 1.3–1.3 m antenna height combination.

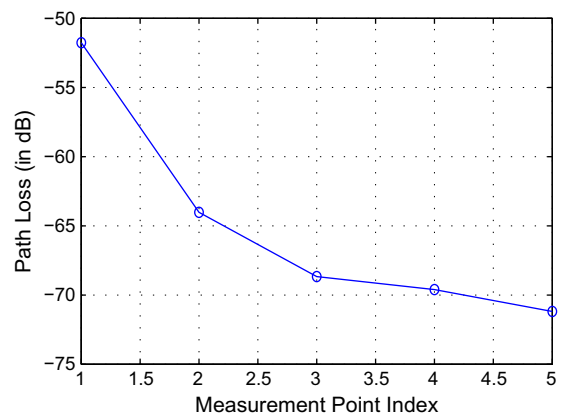


Fig. 9. Indoor U-turn path loss measurement results with 1.3–0.4 m antenna height combination.

Test statistics of the amplitude distribution of indoor environment under LOS are tabulated in Table 1.3. As can be seen, Weibull is the best fitting distribution, with the Rice and Gamma distributions being the next best. NLOS statistics for the indoor environment are given in Table 1.4. In this case, Rayleigh is seen to be the best fitting distribution, with the Weibull and Gamma distributions being the next best.

5. Discussion and comparative analysis

This section provides a comparative analysis of both environments. First, key findings of the parameters described in Section 2 are summarized; next, the focus will be shifted on turn measurement results.

Considering solely n , waveguide effect is seen in both environments for LOS measurements by yielding lower values than that of free space. However, the straight corridor results for indoor measurements provide less loss compared to those for mine measurements. This stems from the fact that the structure of mine is relatively rougher and more irregular. Evidently, this roughness combined with irregularity along with materials covering the mine walls leads to a greater n in mines implying greater loss.

Another key finding is the relationship between n and antenna heights and impact of this relationship on different environments. In comparative analysis, there are four cases to be considered which are obtained by two different antenna height (*i.e.*, high transmitter–high receiver and high transmitter–low receiver antenna) combinations in two different (*i.e.*, underground mine and indoor) environments. It is observed that changing antenna height does not affect drastically the n for indoor, which is in conformity with majority of the results presented in the literature as stated in Section 4.3. However, there are a few studies in the literature for indoor wideband measurements of different antenna heights reporting drastic change in n [30].⁴ On the other hand, according to the results presented in this study, changing antenna height results significant path loss change in underground mines. In this regard, the underground mine in which the measurements were collected behaves different from regular indoor environment in terms of path loss–antenna height relationship. Furthermore, it must be emphasized that, we performed another experiment in which off-the-shelf WLAN products were used in order to control⁵ a rescue robot along a straight corridor in another underground coal mine with a high transmitter–low receiver antenna combination [31]. However, it is fallacious to draw a general conclusion about

the relationship between path loss and antenna height difference by solely considering a few underground mine measurement results. This also makes comparison of underground mines with indoor environments very difficult when path loss exponent and antenna height differences are investigated together.

Results also show that there is no significant frequency-dependent path loss observed in either measurement campaigns over the bandwidth selected. This is not surprising, because frequency-dependent path loss can be observed clearly when the measured spectrum is on the order of GHz width. Nonetheless, one should keep in mind that when the type of mine changes, these behaviors might completely change due to the electromagnetic properties of the material inside mines [20].

When delay statistics are of interest, it is observed that underground mine measurements exhibit significantly longer maximum excess delay and RMS delay spread values. This is a direct consequence of longer corridors present in the underground mine from which the measurements were taken. However, amplitudes of the first coming paths in both environments can be described with the same distributions for both LOS/NLOS conditions implying a strong resemblance in terms of fading characteristics due to very strong structural similarities of both environments.

Apart from the key parameters described earlier, turn measurements are very important for wireless communications in both underground mine and regular indoor environments, since the signal power changes significantly in angled corridors with curvature. The behavior of signals in turns can provide very valuable information about designing and deploying a proper network. In underground mine galleries as well as in regular indoor corridors, the U-turn is one of the most prominent path structures. U-turn measurements are extended version of angle turn measurements, since they include one extra turn after completing the first one.

Measurement results in the mine environment for high transmitter–high receiver antenna height combination are plotted in Fig. 5. As soon as the first turn is made, namely, moving from the 7th to the 8th measurement point, a 6 dB loss is seen. While the receiver is moving inside the L-shape, the first couple of measurement points exhibit the largest loss. However, when the second turn is made to complete the “U” shape by moving from the 13th to the 14th measurement point, the loss is found not to be as significant as the loss between 7th and 8th measurement point (*i.e.*, first turn in the U shape). This is not surprising since the turning capability of electromagnetic waves diminishes when there is a second turn to complete the U-shape. Results obtained from indoor environment are very similar. Fig. 8 shows the same measurement carried out in the regular indoor environment. As soon as the first turn is made, which corresponds to the 2nd measurement point, a 6 dB loss is seen. The second turn, which corresponds to the 6th measurement point, leads to a 4 dB loss while the loss between measurements performed in the farther straight part of the U-shape becomes insignificant. As can be seen from both plots, there is a strong resemblance between two environments in terms of U-turn measurements. However, one should note that the loss

⁴ Note that specifically [30] focuses on 60 GHz band rather than UHF band. Nonetheless, [30] reports that the impact of the antenna height differences on path loss exponent is quite significant.

⁵ In [31], the robot was commanded to move along the mine tunnel while sending the video captured in real time back to control station during its journey. The communication was established, again, by a high transmitter–low receiver antenna combination where high antenna was connected to the control station governing the robot movements, whereas low antenna was placed onto the robot crawling. We maintained the communication successfully up to 1000 ft, which points out a very low power level loss in straight tunnels of underground coal mines being in conformity with the results presented in this paper.

occurred in underground mine when completing the U-shape turn is greater than that in indoor measurements. This difference is emanated from the structures of the walls. Although turns are U-shaped in both environments, radio waves still can penetrate the walls in indoor environment to some extent due to its structure, whereas they cannot pass through in underground mine due to rough wall structure of a coal mine.

The same measurement was performed for the high transmitter–low receiver antenna height combination as well. The results for the mine measurement are plotted in Fig. 5. When the first turn is completed, the loss observed is 8 dB which is higher than the value obtained from the high transmitter–high receiver antenna height combination. Similar behavior is observed in the indoor environment. The loss observed with high transmitter–low receiver antenna height combination after the completion of the first turn is approximately 12 dB as can be seen in Fig. 9. This, again, is greater than the loss observed with the high transmitter–high receiver antenna height combination. In short, the turn loss observed in both of the environments is found to be greater with the high transmitter–low receiver antenna height combination.

Although curvature of corridors is rare in indoor environments, it is very common in underground mines. These sorts of corridors are not straight; however, they allow optical LOS to some extent. The main difference is that the turn is not very sharp, unlike the case of L- and/or U-shape corridors. In order to see the behavior of the received signal power, a curvature test was performed. Results for high transmitter–high receiver antenna height combination are shown in Fig. 6. As can be seen, after the first eight measurement points the signal power increases. This might be caused by the waveguide effect. Another interesting point is that a significant drop occurs at the 12th measurement point although LOS is still maintained at this point. LOS is actually lost at the 15th measurement point. This stems from the fact that although the optical LOS is maintained at the 12th measurement point, the radio waves undergo scattering and diffraction due to the bending point of the curvature yielding an OLOS propagation. Fig. 6 shows the curvature test results for the high transmitter–low receiver antenna height combination too. They follow a similar pattern to that of high transmitter–high receiver antenna height combination. The only difference is in the average received signal power for the first NLOS measurement points, *i.e.*, 12th point. As can be seen, from that point on, average received signal power loses its significance and cannot be distinguished from high transmitter–high receiver antenna height combination.

The last set of measurements in the mine was performed to see the change in path loss for a low transmitter–low receiver antenna height combination in a straight corridor. However, due to time restrictions on mine access, enough statistics could not be collected for this set of measurements. Therefore, the authors avoid making any general comments regarding the path loss measurements of this combination. This antenna height combination was not studied for the indoor environment.

6. Concluding remarks and future directions

This work presents wireless channel measurements that were taken from an active coal mine Jim Walter Resources Inc., mine number 4, in Brookwood, Alabama and a regular indoor channel at Engineering building ENB-118, USF, Tampa, FL. The measurements were performed over a wideband, which covers the interval 850–950 MHz. Studies that focus on propagation characteristics of mines are not vast in the literature due to the restrictions on access and security. Therefore, this work focuses on a band which is not evaluated in detail in spite of its very good propagation characteristics. Radio propagation in both environments is examined, which includes path loss, delay spread, and path amplitude distributions. Besides, signal power measurements in special mine structures such as angle and U-turn (that also covers right-angle turn) are investigated and compared to each other. In addition, to the best knowledge of authors, this paper provides path loss results of different antenna height combinations in mine measurements for the first time in the literature. Based on the results, it is observed that radio propagation in mines exhibits very similar characteristics to those in regular indoor environments. Although underground mines are very harsh environments and have extreme characteristics such as being under the ground, prone to probable explosions, roof falls, collapses, and so on, they still bear strong resemblance to regular environments, since they have long hallways and intersections as in university buildings. This is very important, because it implies that most of the off-the-shelf wireless communication products can be used either directly or with minor modifications in mines for day-to-day and/or rescue operations [31]. However, the relationship between path loss exponent and antenna height is the main distinction between the two environments.

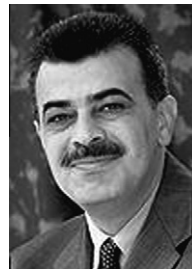
Underground mines can be considered as a transition stage which is between regular and disaster environments. Understanding the radio propagation characteristics in mines will help researchers to model the propagation in disaster environments via well-understood and already settled down regular environments. In this study, it is shown that most of the critical wireless channel parameters exhibit similar behaviors in both environments. However, in order to draw a solid conclusion regarding the resemblance and distinctions between the two environments, the same measurement procedures need to be performed in different mines of different types. This way, not only the complex propagation characteristics of mines due to their special structures is understood better, but also it is possible to have more comprehensive models which allow having generic wireless products working seamlessly in both environments.

Acknowledgements

This work is supported by Mine Safety and Health Administration (MSHA).

References

- [1] R. Bultitude, Measurements of wideband propagation characteristics for indoor radio with predictions for digital system, in: Proceedings of the Wireless '90 Conference, vol. 2, 1990.
- [2] A.A.M. Saleh, R.A. Valenzuela, A statistical model for indoor multipath propagation, IEEE Communications Magazine SAC-5 (1987) 128–137.
- [3] C.C. Huang, R. Khayata, Delay spreads and channel dynamics measurements at ISM bands, in: Proceedings of the IEEE International Conference Communication, ICC '92, 1992, pp. 1222–1226.
- [4] T.S. Rappaport, Characterization of UHF multipath radio channels in factory buildings, IEEE Communications Magazine 37 (1989) 1058–1069.
- [5] T. Takeuchi, M. Sako, S. Yoshida, Multipath delay estimation for indoor wireless communication, in: Proceedings of the IEEE Vehicular Technical Conference, VTC'90, 1990, pp. 401–406.
- [6] Emergency Communication and Tracking Committee, Underground Communication and Tracking Systems Tests at CONSOL Energy Inc., McElroy Mine, Report of findings, Mine Safety and Health Administration (June 13, 2006).
- [7] C.L. Colburn, C.M. Bouton, H.B. Freeman, Underground signaling with radio sets, U.S. Bureau Mines Rep. Inv. 2407.
- [8] J.J. Jakosky, Radio as a method of underground communication in mines, U.S. Bureau Mines Rep. Inv. 2599.
- [9] J.J. Jakosky, Factors retarding transmission of radio signals underground, and some further experiments and conclusions, U.S. Bureau Mines Rep. Inv. 2561.
- [10] A.S. Eve, D.A. Keys, F.W. Lee, The penetration of rock by electromagnetic waves at audio frequencies, in: Proceedings of the IRE, vol. 17, 1929, pp. 2072–2074.
- [11] E.A.J. Marcatili, R.A. Schmeltzer, Hollow metallic and dielectric waveguides for long distance optical transmission and lasers (long distance optical transmission in hollow dielectric and metal circular waveguides, examining normal mode propagation), Bell System Technical Journal 43 (1964) 1783–1809.
- [12] J.I. Glaser, Attenuation and guidance of modes on hollow dielectric waveguides, IEEE Transactions on Microwave Theory Techniques MTT-17 (1969) 173–174.
- [13] S.F. Mahmoud, J.R. Wait, Guided electromagnetic waves in a curved rectangular mine tunnel, Radio Science 9 (1974) 567–572.
- [14] A.E. Goddard, Radio propagation measurements in coal mines at UHF and VHF, in: Proceedings on Through-the-Earth Electromagnetics Workshop, Golden, CO, 1973.
- [15] M. Liénard, P. Degauque, Mobile telecommunication in mine: characterization of the radio channel, in: Proceedings of the 8th Mediterranean Electrotechnical Conference, MELECON '96, vol. 3, 1996, pp. 1663–1665.
- [16] M. Liénard, P. Degauque, Natural wave propagation in mine environments, IEEE Transactions on Antennas and Propagation 48 (9) (2000) 1326–1339.
- [17] A. Benzakour, S. Affès, C. Despains, P.-M. Tardif, Wideband measurements of channel characteristics at 2.4 and 5.8 GHz in underground mining environments, in: Proceedings of the IEEE 60th Vehicular Technology Conference, vol. 5, 2004, pp. 3595–3599.
- [18] C. Nerguizian, C.L. Despains, S. Affès, M. Djadel, Radio-channel characterization of an underground mine at 2.4 GHz, IEEE Transactions on Wireless Communications 4 (5) (2005) 2441–2453.
- [19] M. Boutin, S. Affès, C. Despains, T. Denidni, Statistical modelling of a radio propagation channel in an underground mine at 2.4 and 5.8 GHz, in: Proceedings of the IEEE 61st Vehicular Technology Conference, VTC 2005, Spring, vol. 1, 2005, pp. 78–81.
- [20] S. Yarkan, S. Güzelgöz, H. Arslan, R.R. Murphy, Underground mine communications: a survey, in: IEEE Communications Surveys and Tutorials, in press.
- [21] T.S. Rappaport, Wireless Communications: Principles and Practice, second ed., Prentice Hall Communications Engineering and Emerging Technologies Series, Prentice-Hall, Inc., NJ, USA, 2002.
- [22] A.F. Molisch, K. Balakrishnan, C.-C. Chong, S. Emami, A. Fort, J. Karedal, J. Kunisch, H. Schantz, U. Schuster, K. Siwiak, IEEE 802.15.4a Channel Model – Final Report, Tech. Rep., IEEE P802.15 Working Group for Wireless Personal Area Networks, 2005.
- [23] S. Yarkan, H. Arslan, Statistical wireless channel propagation characteristics in underground mines at 900 MHz, in: Proceedings of IEEE MILCOM, Orlando, FL, USA, 2007.
- [24] S. Yarkan, S. Güzelgöz, H. Arslan, Wireless channel propagation characteristics in underground mines: a statistical analysis and a radio controlled robot experiment, in: Proceedings of the Second IEEE International Conference on Wireless Communications in Underground and Confined Areas (ICWCUA), Val-d'Or, Canada, 2008.
- [25] D.A. Hawbaker, T.S. Rappaport, Indoor wideband radiowave propagation measurements at 1.3 GHz and 4.0 GHz, Electronics Letters 26 (21) (1990) 1800–1802.
- [26] T.S. Rappaport, D.A. Hawbaker, Wide-band microwave propagation parameters using circular and linear polarized antennas for indoor wireless channels, IEEE Transactions on Communications 40 (2) (1992) 240–245.
- [27] V. Hovinen, M. Hämäläinen, T. Pätsi, Ultra wideband indoor radio channel models: preliminary results, in: IEEE Conference on Ultra Wideband Systems and Technologies Digest of Technical Papers, Baltimore, MD, USA, 2002, pp. 75–79.
- [28] K. Pahlavan, R. Ganesh, Statistical characterization of a partitioned indoor radio channel, in: Proceedings of the IEEE International Conference Communication, ICC '92, 1992, pp. 1252–1256.
- [29] S.E. Alexander, Radio propagation within buildings at 900 MHz, Electronics Letters 18 (21) (1982) 913–914.
- [30] H. Yang, M.H. Herben, P.F. Smulders, Channel measurement and analysis for the 60 GHz radio in a reflective environment, in: Proceedings of the 8th International Symposium on Wireless Personal Multimedia Communications (WPMC'05), Aalborg, Denmark, 2005, pp. MA7-4 P.VI-475–MA7-4 P.VI-478.
- [31] R.R. Murphy, R. Shoureshi, H.W. Arnold, H. Arslan, J. Burke, L.J. Greenstein, D.K. Killinger, C.W. Lundgren, A.J. Rustako, S. Stover, Analysis of Viability and Feasibility of Current and Emerging Mining Communication and Mine Rescue Technologies, Final Report, Institute for Safety, Security, Rescue Technology, University of South Florida, Tampa, FL, USA, March 2008.



Dr Khalid A. Qaraqe (M'97–S'00) was born in Bethlehem. He received the B.S. degree in EE from the University of Technology, Baghdad in 1986, with honors. He received the M.S. degree in EE from the University of Jordan, Jordan, in 1989, and he earned his Ph.D. degree in EE from Texas A & M University, College Station, TX, in 1997. From 1989 to 2004 Dr Qaraqe has held a variety positions in many companies and he has over 12 years of experience in the telecommunication industry. He has worked for Qualcomm, Enad Design Systems, Cadence Design Systems/Tality Corporation, STC, SBC and Ericsson. He has also worked on numerous GSM, CDMA, WCDMA projects and has experience in product development, design, deployments, testing and integration. Dr Qaraqe joined the department of Electrical Engineering of Texas A & M University at Qatar, in July 2004, where he is now associate professor. Dr Qaraqe research interests include communication theory and its application to design and performance, analysis of cellular systems and indoor communication systems. Particular interests are in the development of 3G UMTS, cognitive radio systems, broadband wireless communications and diversity techniques.



Serhan Yarkan received his both B.S. and M.Sc. degrees in Computer Science from Istanbul University, Istanbul, Turkey in 2001 and 2003, respectively. He received his Ph.D. degree in 2009 from Department of Electrical Engineering at the University of South Florida. He is currently with Department of Computer and Electrical Engineering at Texas A & M University, College Station, TX, as a post-doctoral research associate. His research interests include statistical signal processing, cognitive radio, wireless propagation channel modeling, cross-layer adaptation and optimization, and interference management in next generation wireless networks.



Sabih Guzelgoz was born in Bursa, Turkey in 1980. He received his B.S. degree in electrical and electronics engineering from Osmangazi University, Eskisehir, Turkey, in 2002. He received his M.S. degree in electronics from the University of York, UK, in 2004. He is currently pursuing his Ph.D. degree in electrical engineering at the University of South Florida. His research interests are wireless propagation channel modeling, digital base-band transceiver algorithms, and application of basic intelligence to cognitive radio networks.



Hüseyin Arslan has received his Ph.D. degree in 1998 from Southern Methodist University, Dallas, TX. From January 1998 to August 2002, he was with the research group of Ericsson Inc., NC, USA. Since August 2002, he has been with Electrical Engineering Dept. of University of South Florida. His research interests are related to advanced signal processing techniques for cross-layer design, networking adaptivity and QoS control for UWB, OFDM-based wireless technologies with emphasis on WiMAX, and cognitive and SDR.